HHS Public Access

Author manuscript

*J Alzheimers Dis*. Author manuscript; available in PMC 2019 April 23.

Published in final edited form as:

*J Alzheimers Dis*. 2018 ; 66(3): 927–934. doi:10.3233/JAD-180592.

# DNA Hypomethylation in Blood Links *B3GALT4* and *ZADH2* to Alzheimer's Disease

**Andy Madrid**[a,b], **Kirk J. Hogan**[c,d,*,1], **Ligia A. Papale**[a], **Lindsay R. Clark**[d,e,f], **Sanjay Asthana**[e,f], **Sterling C. Johnson**[d,e,f], and **Reid S. Alisch**[a,1]

[a]Department of Psychiatry, University of Wisconsin School of Medicine and Public Health, Madison, WI, USA

[b]Neuroscience Training Program, University of Wisconsin School of Medicine and Public Health, Madison, WI, USA

[c]Department of Anesthesiology, University of Wisconsin School of Medicine and Public Health, Madison, WI, USA

[d]Wisconsin Alzheimer's Institute, University of Wisconsin School of Medicine and Public Health, Madison, WI, USA

[e]Wisconsin Alzheimer's Disease Research Center, University of Wisconsin School of Medicine and Public Health, Madison, WI, USA

[f]Geriatric Research Education and Clinical Center, William S. Middleton Memorial Veterans Hospital, Madison, WI, USA

## Abstract

Differentially methylated positions (DMPs) between persons with and without late-onset Alzheimer's disease (LOAD) were observed at 477 of 769,190 loci in a plurality of genes. Of these, 17 were shared with DMPs identified using clinical LOAD markers analyzed independently as continuous variables comprising Rey Auditory Verbal Learning Test scores, cerebrospinal fluid total tau (t-tau) and phosphorylated tau 181 (p-tau$_{181}$) levels, and t-tau/Aβ1–42 (Aβ$_{42}$), p-tau$_{181}$/Aβ$_{42}$, and Aβ$_{42}$/Aβ1–40 (Aβ$_{40}$) ratios. In patients with LOAD, 12 of the shared 17 DMPs were hypomethylated in *B3GALT4* (Beta-1,3-galatcosyltransferase 4) (EC 2.4.1.62), and5 were hypomethylated in *ZADH2* (Prostaglandin reductase 3) (EC 1.3.1.48).

### Keywords

Amyloid; DNA methylation; late-onset Alzheimer's disease; tau proteins

*Correspondence to: Kirk J. Hogan, Department of Anesthesiology, Wisconsin Alzheimer's Institute, University of Wisconsin-Madison School of Medicine and Public Health, Madison, WI, USA. Tel.: +1 608 263 8100; khogan@wisc.edu.

[1]These authors contributed equally to this work.

SUPPLEMENTARY MATERIAL

The supplementary material is available in the electronic version of this article: http://dx.doi.org/10.3233/JAD-180592.

Authors' disclosures available online (https://www.j-alz.com/manuscript-disclosures/18-0592r3).

## INTRODUCTION

Covalent addition of a methyl group at position 5 of the nucleotide cytosine generates 5-methylcytosine (5mC) that is most often observed in the human genome adjacent to a guanine in a CpG dinucleotide. Cytosine methylation is less common in dense clusters of CpG dinucleotides referred to as CpG islands that participate in the regulation of gene transcription when located in promoter regions [1]. Fluctuations in 5mC levels across the genome are observed over the lifespan in association with cognitive aging in neurodegeneration, and with changes in learning and memory [2–4]. Variations in 5mC abundance have been identified in postmortem brain tissues of late-onset Alzheimer's disease (LOAD) patients in genes that correlate with LOAD susceptibility. Recent epigenome-wide association studies (EWAS) report differential methylation in known and newly recognized LOAD genes, thereby underscoring the utility of EWAS in disclosing novel genes and pathways associated with LOAD pathogenesis [5–8]. As an alternative to the study of donor brain tissues, investigation of DNA methylation in accessible peripheral tissues may provide an opportunity to improve clinical diagnosis and estimates of prognosis, and to guide personalized treatment of LOAD [9]. To identify differences in the distribution of 5mC associated with LOAD, we extracted genomic DNA from the whole blood of 45 LOAD patients and 39 matched controls, and used the Illumina HumanMethylationEPIC array platform to interrogate >850,000 methylated sites spanning the genome for the presence of differentially methylated positions (DMPs) that distinguish persons with and without LOAD.

## MATERIALS AND METHODS

### Participants

Inclusion of human participants in this study was approved by the University of Wisconsin-Madison institutional review board, and all participants provided informed consent.

Participants were 45 patients with a clinical diagnosis of LOAD based on NIA-AA criteria, and 39 persons without cognitive impairment matched for age, sex, and education who are enrolled in the longitudinal Wisconsin Alzheimer's Disease Research Center (WADRC) clinical core. Participants in the WADRC clinical core are evaluated annually with a panel of cognitive performance tests. Cognitive status is determined by a consensus conference panel based on National Institute on Aging-Alzheimer's Association criteria [10, 11].

### Neuropsychological assessment

Measures of learning and memory (Rey Auditory Verbal Learning Test (RAVLT), Total Trials and Delayed Recall), and executive function (Trail Making Test Part B (TMT-B)) were included based on prior meta-analyses indicating that these cognitive domains demonstrate significant decline and association with LOAD biomarkers [12–16].

### Cerebrospinal fluid (CSF) amyloid and tau

CSF was collected in the morning after a minimum 12-h fast, as previously described [17]. Samples were sent to the Clinical Neurochemistry Laboratory at the Sahlgrenska Academy

of the University of Gothenburg, Sweden, and analyzed according to protocols approved by the Swedish Board of Accreditation and Conformity Assessment using one batch of reagents (intra-assay coefficients of variation <10%) for each of two batches. CSF samples were assayed for total tau (t-tau), phosphorylated tau 181 (p-tau$_{181}$), Aβ1–42 (Aβ$_{42}$), and Aβ1–40 (Aβ$_{40}$) using commercially available ELISA methods (INNOTEST assays, Fujirebio, Ghent, Belgium), and (Aβ$_{42}$/Aβ$_{40}$) ratios (Triplex assays, MSD Human Aβ[beta] Peptide Ultra-Sensitive Kit, Meso Scale Discovery, Gaithersburg, MD). Batch-to-batch conversions were performed as previously described [17].

## Blood genomic DNA methylation

Whole blood was collected into a 10 ml EDTA tube and mixed by rocking for 5 min. Blood was then aliquoted into 2 × 5 ml and frozen in a 20°C freezer overnight, then moved to a −80°C freezer. Samples were thawed and genomic DNA was extracted using the Gentra Puregene Blood kit, following the manufacturer's protocol (Qiagen, Hilden, Germany). Extracted genomic DNA was resolved on a 1% agarose gel to verify that the DNA was of high molecular weight, and was quantified using Qubit™ (Qiagen, Hilden, Germany). Five hundred nanograms of genomic DNA were sodium bisulfite-treated to convert unmethylated cytosines to uracils using the EZ DNA Methylation-Gold™ kit (Zymo Research, Irvine, CA, USA). The converted DNA was purified and prepared for analysis on the Illumina HumanMethylationEPIC BeadChips™ according to manufacturer protocols (Illumina, San Diego, CA, USA). In brief, the bisulfite-converted DNA was amplified, fragmented, and hybridized to the HumanMethylationEPIC pool of allele-differentiating oligonucleotides to ensure an equal and random placement of participants and controls on each beadchip. After serial extension, ligation, and cleanup reactions, the DNA was labeled with a fluorescent dye. The labeled DNA was then scanned using an Illumina iScan array scanner. Image analysis, and signal determinations were performed using the GenomeStudio software, Methylation Module (Illumina, San Diego, CA, USA).

## Preprocessing HumanMethylationEPIC data

Raw intensity data files were imported into R package *minfi* to assess sample quality, to calculate the detection *p*-value of each tested probe, and to estimate blood cell counts for each sample [18]. Probes were background- and control-corrected, followed by subset-quantile within array normalization to correct for probe-type bias [18–20]. Probes were removed from further analysis if: one sample or more exhibited a detection *p*-value >0.01; the probe contained a single nucleotide polymorphism (SNP); the probe reported methylation at a SNP; the probe was derived from a sex chromosome; the probe measured methylation at a cytosine followed by a nucleotide other than guanine; or the probe is a cross-reactive probe. With these filtration criteria, 97,647 probes were discarded and 769,190 probes were available for further analysis.

## Statistical analyses

Demographic characteristics from participants with and without LOAD were compared using T-tests with a significance level of $p < 0.05$ adopted for all comparisons. Table 1 indicates those with significance. Methylation levels (i.e., beta-values) were calculated in *minfi* as the ratio of methylated to total signal (i.e., beta-value = methylated signal/

(methylated signal + unmethylated signal +100)), where beta-values range from 0 (fully unmethylated) to 1 (fully methylated). Beta values were further converted to *M*-values (i.e., logit-transformed beta-values) for differential analysis to generate *M*-values appropriate for statistical testing. Linear regression for each tested CpG using a multivariate model was employed using R package *limma* [21] and all discrete (i.e., LOAD versus no-LOAD) and continuous variables were treated as the independent variable, while methylation level was the dependent variable. A model adjusted for LOAD versus no-LOAD, sex, age, identification number of the HumanMethylationEPIC array (N = 12), and white blood cell counts (i.e., granulocytes, monocytes, natural killer, B-cell, CD8T, and CD4T lymphocytes) was used for regression [18, 22]. To assess systematic bias of the linear regression model, the genomic inflation factor was calculated for the obtained *p*-values, yielding a genomic inflation factor of 1.01, thereby suggesting no bias in these methods [23]. All methylation data was subjected to surrogate variable analysis (R package sva). Because methylation levels of immediately flanking probes tested by array-based platforms may exhibit dependence upon one another, and because corrections for multiple testing such as the Benjamini-Hochberg false discovery rate may be inefficient under a varying dependence structure, the R package *NHMMfdr* was used to detect the adjusted local index of significance (aLIS), an extension of adjusted *p*-values, for each probe by first converting all *p*-values to z-scores, followed by using a nonparametric Gaussian mixture distribution with one mixture component, and all other parameters set to default [24]. An aLIS threshold of <0.05 was used to identify differentially methylated loci. The same multivariate model was used when testing the continuous variables of interest: RAVLT, Total Trials and Delayed Recall scores, and TMT-B scores ($n$ = 38 LOAD, $n$ = 39 no-LOAD), and CSF t-tau, p-tau$_{181}$, A$\beta_{42}$, A$\beta_{40}$ levels and t-tau/A$\beta_{42}$, p-tau/A$\beta_{42}$, and A$\beta_{42}$/A$\beta_{40}$ ratios ($n$ = 16 LOAD, $n$ = 24 no-LOAD).

## RESULTS

### Participant characteristics

Table 1 provides demographic characteristics of participants with and without LOAD. LOAD and no-LOAD participants did not differ in age and sex. Patients with LOAD had 2 fewer years of educational attainment. As expected, CSF values differed between groups.

### Genome-wide DNA methylation

Of 769,190 loci tested, 477 CpG positions were differentially methylated (Supplementary Table 1). Classification of the differentially methylated positions to the nearest gene revealed 106 DMP-associated genes, including 21 hypermethylated loci and 97 hypomethylated loci. Twelve genes contained more than one DMP that were hypermethylated and hypomethylated at distinct genomic positions. The mean distance between adjacent hypermethylated and hypomethylated DMPs in the same gene was >500 kilobases. A proportion of DMP-associated genes and their products have been noted by others to participate in LOAD pathogenesis including *B3GALT4, FLOT1, OXT,* and *DLG2* [7, 25–27].

Each comparison of 6 continuous variables comprising RAVLT scores, and CSF t-tau and p-tau$_{181}$ levels, or t-tau/A$\beta_{42}$, p-tau$_{181}$/A$\beta_{42}$, or A$\beta_{42}$/A$\beta_{40}$ ratios yielded a unique set of DMPs. Of the 477 DMPs that distinguished participants with and without LOAD, 17 DMPs were also shared among the 6 continuous variables (Fig. 1). In LOAD patients, 12 of the shared 17 DMPs were hypomethylated in *B3GALT4* (Beta-1,3-galatcosyltransferase 4) (EC 2.4.1.62), and 5 were hypomethylated in *ZADH2* (Prostaglandin reductase 3) (EC 1.3.1.48) (Fig. 2). Differential levels of DNA methylation at 7 of 7 DMPs at the *B3GALT4* locus observed using the HumanMethylationEPIC array was confirmed by pyrosequencing, with a mean correlation coefficient of >0.9 for the 7 DMP sites. When analyzed as continuous variables, no DMPs associated with TMT-B scores and A$\beta_{42}$ levels were observed that distinguish participants with and without LOAD, and that were shared between the other 6 continuous variables. No surrogate variables were identified in the data, indicating that the variables used in the model (e.g., LOAD versus no-LOAD) accounted for the preponderance of the observed variance, and that latent confounders (e.g., education) were not a source of bias or noise.

## DISCUSSION

Genome-wide DNA methylation analysis reveals that LOAD-related DMPs are located throughout the human genome in peripheral blood. In LOAD patients, 17 hypomethylated DMPs in *B3GALT4* and *ZADH2* are shared with DMPs associated with memory performance, and CSF levels of Aβ and tau. *B3GALT4* encodes the enzyme Beta-1,3-galactosyltransferase 4, a type II membrane-bound glycoprotein crucial for the biosynthesis of GM1. GM1 is a ganglioside on the surface of vertebrate cells that participates in the regulation of synaptic transmission in the brain [28–30]. GM1 and other components of the ganglioside biosynthesis pathway are associated with LOAD onset and progression, neuronal cell survival, and neurotoxicity [31–35]. A critical event leading to synaptic failure associated with LOAD is perturbation of neuronal cell membranes resulting from the generation of porelike structures that jeopardize cell integrity [36]. Synaptotoxicity arises at least in part from lipid raft aggregation of Aβ Aβ [36]. Gangliosides including GM1 are concentrated in lipid rafts and interact with Aβ, thereby supporting a role for GM1 and Aβ interactions in disruption of neuronal membrane integrity and dysregulation of GM1 biosynthesis by aberrant *B3GALT4* expression as contributors to LOAD pathogenesis [37, 38]. A previous study of DNA methylation alterations in the superior temporal gyrus of postmortem LOAD brain samples reported 53 hypermethylated positions in *B3GALT4* [7]. Twelve of the 53 were those hypomethylated in the present study suggesting an inverse cross-tissue (i.e., brain and blood) correlation with LOAD.

*ZADH2* encodes the enzyme zinc binding alcohol dehydrogenase domain containing 2, also referred to as prostaglandin reductase 3 (PGR3). PGR3 is a member of the cyclooxygenase-prostaglandin pathway with a high affinity for 15-keto-PGE2-α [39–41]. The cyclooxygenase-prostaglandin pathway is associated with LOAD risk, particularly PGE2 [42]. Diverse members of the pathway promote pro-inflammatory and anti-inflammatory responses through cell-type-specific G-protein coupled receptors with inhibition of cyclooxygenases reported to decrease LOAD risk [43–46].

Two online blood-brain DNA methylation comparison instruments were used to interrogate the 12 *B3GALT4* DMPs that correlate with LOAD expression in our data. Lower levels of *B3GALT4* DNA methylation in our samples of white blood cells from living patients with LOAD were observed in comparison to samples of postmortem brain tissues from patients who died from LOAD that were used to generate the online instruments [47,48]. Other investigators similarly report discordant DNA methylation profiles between blood and brain tissues associated with other neurological disorders [49–51]. With regard to the *ZADH2* locus, 4 of the 5 DMPs that we report were compared with data from the 450 K array used to generate the BECon analysis and the Blood Brain DNA Methylation Comparison Tool [47, 48]. The 4 DMPs show similar levels of DNA methylation between blood and tissue from diverse brain regions. The 5th *ZADH2* DMP that we report to be differentially methylated between patients with LOAD and participants without LOAD is a novel probe on the 850K array, and is not interrogated by two online tools. The interpretation and implications of these findings remain to be elucidated. Chouliaras et al. have recently described DMPs in *HLA-DPA1/HLA-DPB1, DRC1, PRKAA2, CACLB, CDH2, RTBDN, ZNF256,* and *SHANK2* genes in the blood of participants with mild cognitive impairment (MCI) based on Montreal Cognitive Assessment (MoCA) scores in comparison to sex-matched cognitively normal participants [52]. No DMPs in blood are shared between these observations in participants with MCI and the results of the present investigation of participants with LOAD, suggesting that progression to LOAD exhibits distinct DMP patterns not associated with MCI. Taken together, these data reinforce the use of blood as an accessible tissue of value in the identification of DMPs associated with dementia onset and progression. Our data lend further support to the role of enzymes in ganglioside and prostaglandin metabolism in the pathogenesis of AD, and may provide novel diagnostic, prognostic and modifiable therapeutic targets.

## Supplementary Material

Refer to Web version on PubMed Central for supplementary material.

## ACKNOWLEDGMENTS

The authors gratefully acknowledge the assistance of researchers and staff at the Wisconsin Alzheimer's Disease Research Center for assistance in recruitment and data collection. The authors thank Ms. Sandra Splinter Bondurant and her associates at the UW Biotechnology Center. This work was supported by NIH grants (ADRC P50 AGO33514) (S.A.) and RO1 AG027161 (S.J.C.), by a University of Wisconsin ADRC pilot award (R.S.A. and K.H.), and by a Ruth L. Kirschstein National Research Service Award (MH113351-02) (A.M.).

## REFERENCES

[1]. Smith ZD, Meissner A (2013) DNA methylation: Roles in mammalian development. Nat Rev Genet 14, 204–220. [PubMed: 23400093]

[2]. Sanchez-Mut JV, Heyn H, Vidal E, Moran S, Sayols S, Delgado-Morales R, Schultz MD, Ansoleaga B, Garcia-Esparcia P, Pons-Espinal M, de Lagran MM, Dopazo J, Rabano A, Avila J, Dierssen M, Lott I, Ferrer I, Ecker JR, Esteller M (2016) Human DNA methylomes of neurodegenerative diseases show common epigenomic patterns. Transl Psychiatry 6, e718. [PubMed: 26784972]

[3]. Day JJ, Sweatt JD (2010) DNA methylation and memory formation. Nat Neurosci 13, 1319–1323. [PubMed: 20975755]

[4]. Day JJ, Childs D, Guzman-Karlsson MC, Kibe M, Moulden J, Song E, Tahir A, Sweatt JD (2013) DNA methylation regulates associative reward learning. Nat Neurosci 16, 1445–1452. [PubMed: 23974711]

[5]. Bakulski KM, Dolinoy DC, Sartor MA, Paulson HL, Konen JR, Lieberman AP, Albin RL, Hu H, Rozek LS (2012) Genome-wide DNA methylation differences between late-onset Alzheimer's disease and cognitively normal controls in human frontal cortex. J Alzheimers Dis 29, 571–588. [PubMed: 22451312]

[6]. Lunnon K, Smith R, Hannon E, De Jager PL, Srivastava G, Volta M, Troakes C, Al-Sarraj S, Burrage J, Macdonald R, Condliffe D, Harries LW, Katsel P, Haroutunian V, Kaminsky Z, Joachim C, Powell J, Lovestone S, Bennett DA, Schalkwyk LC, Mill J (2014) Methylomic profiling implicates cortical deregulation of ANK1 in Alzheimer's disease. Nat Neurosci 17, 1164–1170. [PubMed: 25129077]

[7]. Watson CT, Roussos P, Garg P, Ho DJ, Azam N, Katsel PL, Haroutunian V, Sharp AJ (2016) Genome-wide DNA methylation profiling in the superior temporal gyrus reveals epigenetic signatures associated with Alzheimer's disease. Genome Med 8, 5. [PubMed: 26803900]

[8]. Coppieters N, Dieriks BV, Lill C, Faull RL, Curtis MA, Dragunow M (2014) Global changes in DNA methylation and hydroxymethylation in Alzheimer's disease human brain. Neurobiol Aging 35, 1334–1344. [PubMed: 24387984]

[9]. Fransquet PD, Lacaze P, Saffery R, McNeil J, Woods R, Ryan J (2018) Blood DNA methylation as a potential biomarker of dementia: A systematic review. Alzheimers Dement 14, 81–103. [PubMed: 29127806]

[10]. Albert MS, DeKosky ST, Dickson D, Dubois B, Feldman HH, Fox NC, Gamst A, Holtzman DM, Jagust WJ, Petersen RC, Snyder PJ, Carrillo MC, Thies B, Phelps CH (2011)The diagnosis of mild cognitive impairment due to Alzheimer's disease: Recommendations from the National Institute on Aging-Alzheimer's Association workgroups on diagnostic guidelines for Alzheimer's disease. Alzheimers Dement 7, 270–279. [PubMed: 21514249]

[11]. McKhann GM, Knopman DS, Chertkow H, Hyman BT, Jack CR Jr., Kawas CH, Klunk WE, Koroshetz WJ, Manly JJ, Mayeux R, Mohs RC, Morris JC, Rossor MN, Scheltens P, Carrillo MC, Thies B, Weintraub S, Phelps CH (2011) The diagnosis of dementia due to Alzheimer's disease: Recommendations from the National Institute on Aging-Alzheimer's Association workgroups on diagnostic guidelines for Alzheimer's disease. Alzheimers Dement 7, 263–269. [PubMed: 21514250]

[12]. Reitan RM (1994) Ward Halstead's contributions to neuropsychology and the Halstead-Reitan Neuropsychological Test Battery. J Clin Psychol 50, 47–70. [PubMed: 8150995]

[13]. Backman L, Jones S, Berger AK, Laukka EJ, Small BJ (2005) Cognitive impairment in preclinical Alzheimer's disease: A meta-analysis. Neuropsychology 19, 520–531. [PubMed: 16060827]

[14]. Hedden T, Oh H, Younger AP, Patel TA (2013) Meta-analysis of amyloid-cognition relations in cognitively normal older adults. Neurology 80, 1341–1348. [PubMed: 23547267]

[15]. Duke Han S, Nguyen CP, Stricker NH, Nation DA (2017) Detectable neuropsychological differences in early preclinical Alzheimer's disease: A meta-analysis. Neuropsychol Rev 27, 305–325. [PubMed: 28497179]

[16]. Schmidt M (1996) Rey Auditory Verbal Learning Test: A Handbook. Western Psychological Services, Los Angeles.

[17]. Clark LR, Berman SE, Norton D, Koscik RL, Jonaitis E, Blennow K, Bendlin BB, Asthana S, Johnson SC, Zetterberg H, Carlsson CM (2018) Age-accelerated cognitive decline in asymptomatic adults with CSF beta-amyloid. Neurology 90, e1306–e1315. [PubMed: 29523644]

[18]. Aryee MJ, Jaffe AE, Corrada-Bravo H, Ladd-Acosta C, Feinberg AP, Hansen KD, Irizarry RA (2014) *minfi:* A flexible and comprehensive Bioconductor package for the analysis of Infinium DNA methylation microarrays. Bioinformatics 30, 1363–1369. [PubMed: 24478339]

[19]. Maksimovic J, Gordon L, Oshlack A (2012) SWAN:Subset-quantile within array normalization for illumina infinium HumanMethylation450 BeadChips. Genome Biol 13, R44. [PubMed: 22703947]

[20]. Wockner LF, Noble EP, Lawford BR, Young RM, Morris CP, Whitehall VL, Voisey J (2014) Genome-wide DNA methylation analysis of human brain tissue from schizophrenia patients. Transl Psychiatry 4, e339. [PubMed: 24399042]

[21]. Ritchie ME, Phipson B, Wu D, Hu Y, Law CW, Shi W, Smyth GK (2015) limma powers differential expression analyses for RNA-sequencing and microarray studies. Nucleic Acids Res 43, e47. [PubMed: 25605792]

[22]. Houseman EA, Accomando WP, Koestler DC, Christensen BC, Marsit CJ, Nelson HH, Wiencke JK, Kelsey KT (2012) DNA methylation arrays as surrogate measures of cell mixture distribution. BMC Bioinformatics 13, 86. [PubMed: 22568884]

[23]. Yang J, Weedon MN, Purcell S, Lettre G, Estrada K, Willer CJ, Smith AV, Ingelsson E, O'Connell JR, Mangino M, Magi R, Madden PA, Heath AC, Nyholt DR, Martin NG, Montgomery GW, Frayling TM, Hirschhorn JN, McCarthy MI, Goddard ME, Visscher PM, Consortium G (2011) Genomic inflation factors under polygenic inheritance. Eur J Hum Genet 19, 807–812. [PubMed: 21407268]

[24]. Kuan PF, Chiang DY (2012) Integrating prior knowledge in multiple testing under dependence with applications to detecting differential DNA methylation. Biometrics 68,774–783. [PubMed: 22260651]

[25]. Hondius DC, van Nierop P, Li KW, Hoozemans JJ, van der Schors RC, van Haastert ES, van der Vies SM, Rozemuller AJ, Smit AB (2016) Profiling the human hippocampal proteome at all pathologic stages of Alzheimer's disease. Alzheimers Dement 12, 654–668. [PubMed: 26772638]

[26]. Yuyama K, Sun H, Sakai S, Mitsutake S, Okada M, Tahara H, Furukawa J, Fujitani N, Shinohara Y, Igarashi Y (2014) Decreased amyloid-beta pathologies by intracerebral loading of glycosphingolipid-enriched exosomes in Alzheimer model mice. J Biol Chem 289, 24488–24498. [PubMed: 25037226]

[27]. Mazurek MF, Beal MF, Bird ED, Martin JB (1987) Oxytocin in Alzheimer's disease: Postmortem brain levels. Neurology 37, 1001–1003. [PubMed: 3587615]

[28]. Sasaki N, Itakura Y, Toyoda M (2015) Ganglioside GM1 contributes to the state of insulin resistance in senescent human arterial endothelial cells. J Biol Chem 290, 25475–25486. [PubMed: 26338710]

[29]. Schnaar RL (2016) Gangliosides of the vertebrate nervous system. J Mol Biol 428, 3325–3336. [PubMed: 27261254]

[30]. Fernandez-Perez EJ, Sepulveda FJ, Peoples R, Aguayo LG (2017) Role of membrane GM1 on early neuronal membrane actions of Abeta during onset of Alzheimer's disease. Biochim Biophys Acta 1863, 3105–3116.

[31]. Fukami Y, Ariga T, Yamada M, Yuki N (2017) Brain gangliosides in Alzheimer's disease: Increased expression of cholinergic neuron-specific gangliosides. Curr Alzheimer Res 14, 586–591. [PubMed: 28124591]

[32]. Matsubara T, Nishihara M, Yasumori H, Nakai M, Yanagisawa K, Sato T (2017) Size and shape of amyloid fibrils induced by ganglioside nanoclusters: Role of sialyl oligosaccharide in fibril formation. Langmuir 33, 13874–13881. [PubMed: 29148800]

[33]. Liang Y, Ji J, Lin Y, He Y, Liu J (2016) The ganglioside GM-1 inhibits bupivacaine-induced neurotoxicity in mouse neuroblastoma Neuro2a cells. Cell Biochem Funct 34, 455–462. [PubMed: 27558076]

[34]. Kracun I, Kalanj S, Cosovic C, Talan-Hranilovic J (1990) Brain gangliosides in Alzheimer's disease. J Hirnforsch 31, 789–793. [PubMed: 2092064]

[35]. Yanagisawa K (2015) GM1 ganglioside and Alzheimer's disease. Glycoconj J 32, 87–91. [PubMed: 25903682]

[36]. Sepulveda FJ, Fierro H, Fernandez E, Castillo C, Peoples RW, Opazo C, Aguayo LG (2014) Nature of the neurotoxic membrane actions of amyloid-beta on hippocampal neurons in Alzheimer's disease. Neurobiol Aging 35, 472–481. [PubMed: 24112789]

[37]. Yanagisawa K, Odaka A, Suzuki N, Ihara Y (1995) GM1 ganglioside-bound amyloid beta-protein (A beta): A possible form of preamyloid in Alzheimer's disease. Nat Med 1, 1062–1066. [PubMed: 7489364]

[38]. Fishman MA, Agrawal HC, Alexander A, Golterman J (1975) Biochemical maturation of human central nervous system myelin. J Neurochem 24, 689–694. [PubMed: 47384]

[39]. Johansson JU, Woodling NS, Shi J, Andreasson KI (2015) Inflammatory cyclooxygenase activity and PGE2 signaling in models of Alzheimer's disease. Curr Immunol Rev 11, 125–131. [PubMed: 28413375]

[40]. Yagami T, Koma H, Yamamoto Y (2016) Pathophysiological roles of cyclooxygenases and prostaglandins in the central nervous system. Mol Neurobiol 53, 4754–4771. [PubMed: 26328537]

[41]. Johansson JU, Woodling NS, Wang Q, Panchal M, Liang X, Trueba-Saiz A, Brown HD, Mhatre SD, Loui T, Andreasson KI (2015) Prostaglandin signaling suppresses beneficial microglial function in Alzheimer's disease models. J Clin Invest 125,350–364. [PubMed: 25485684]

[42]. Woodling NS, Andreasson KI (2016) Untangling the web: Toxic and protective effects of neuroinflammation and PGE2 signaling in Alzheimer's disease. ACS Chem Neurosci 7, 454–463. [PubMed: 26979823]

[43]. In t' Veld BA, Ruitenberg A, Hofman A, Launer LJ, van Duijn CM, Stijnen T, Breteler MM, Stricker BH (2001) Nonsteroidal antiinflammatory drugs and the risk of Alzheimer's disease. N Engl J Med 345, 1515–1521. [PubMed: 11794217]

[44]. Stewart WF, Kawas C, Corrada M, Metter EJ (1997) Risk of Alzheimer's disease and duration of NSAID use. Neurology 48, 626–632. [PubMed: 9065537]

[45]. Zandi PP, Anthony JC, Hayden KM, Mehta K, Mayer L, Breitner JC, Cache County Study Investigators (2002) Reduced incidence of AD with NSAID but not H2 receptor antagonists: The Cache County Study. Neurology 59, 880–886. [PubMed: 12297571]

[46]. McGeer PI, Guo JP, Lee M, Kennedy K, McGeer EG (2018) Alzheimer's disease can be spared by nonsteroidal antiinflammaotry drugs. J Alzheimers Dis 62, 1219–1222. [PubMed: 29103042]

[47]. Hannon E, Lunnon K, Schalkwyk L, Mill J (2015) Interindividual methylomic variation across blood, cortex, and cerebellum: Implications for epigenetic studies of neurological and neuropsychiatric phenotypes. Epigenetics 10, 1024–1032. [PubMed: 26457534]

[48]. Edgar RD, Jones MJ, Meaney MJ, Turecki G, Kobor MS (2017) BECon: A tool for interpreting DNA methylation findings from blood in the context of brain. Transl Psychiatry 7, e1187. [PubMed: 28763057]

[49]. Farre P, Jones MJ, Meaney MJ, Emberly E, Turecki G, Kobor MS (2015) Concordant and discordant DNA methylation signatures of aging in human blood and brain. Epigenetics Chromatin 8, 19. [PubMed: 25977707]

[50]. Walton E, Hass J, Liu J, Roffman JL, Bernardoni F, Roessner V, Kirsch M, Schackert G, Calhoun V, Ehrlich S (2016) Correspondence of DNA methylation between blood and brain tissue and its application to schizophrenia research. Schizophr Bull 42, 406–414. [PubMed: 26056378]

[51]. Yu L, Chibnik LB, Yang J, McCabe C, Xu J, Schneider JA, D Jager PL, Bennett (2016) Methylation profiles in peripheral blood CD4+ lymphocytes versus brain: The relation to Alzheimer's disease pathology. Alzheimers Dement 12, 942–951. [PubMed: 27016692]

[52]. Chouliaras L, Kenis G, Visser PJ, Scheltens P, Tsolaki M, Jones RW, Kehoe PG, Graff C, Girtler NG, Wallin AK, Rikkert MO, Spiru L, Elias-Sonnenschein LS, Ramakers IH, Pishva E, van Os J, Steinbusch HW, Verhey FR, van den Hove DL, Rutten BP (2015) DNMT3A moderates cognitive decline in subjects with mild cognitive impairment: Replicated evidence from two mild cognitive impairment cohorts. Epigenomics 7, 533–537. [PubMed: 26111027]

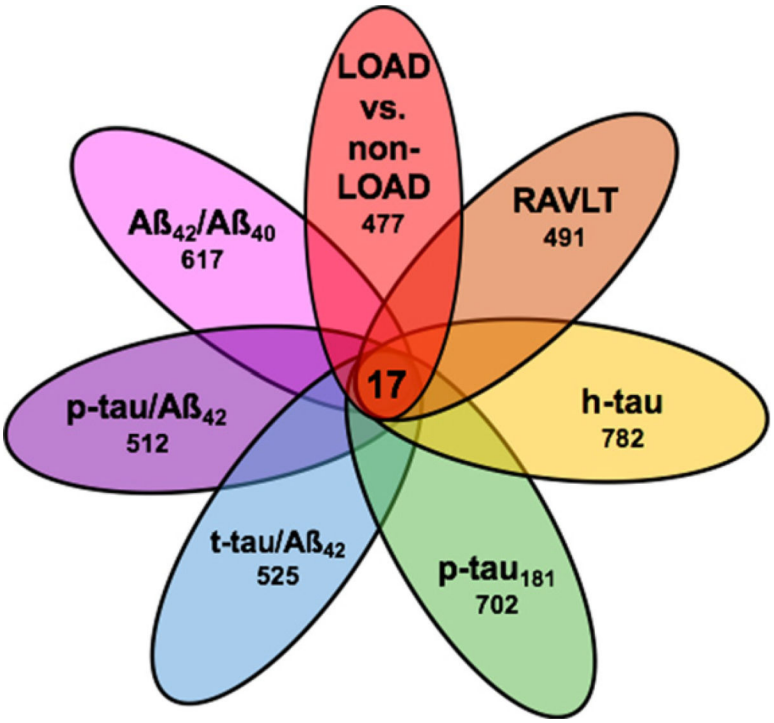


**Fig. 1.**

Differentially methylated positions (DMPs) in white blood cell DNA between LOAD patients and matched no-LOAD persons. The Venn diagram depicts differentially methylated CpG sites within each of 7 comparison groups (LOAD versus non-LOAD (red), Rey Auditory Verbal Learning Test (RAVLT) scores (orange), h-tau (yellow), and p-tau$_{181}$ (green) levels, and t-tau/A$\beta_{42}$(blue), p-tau/A$\beta_{42}$ (purple), and A$\beta_{42}$/A$\beta_{40}$ (pink) ratios. Numerical values within each oval are the number of DMPs identified for each variable. Seventeen DMPs were shared between all comparisons.

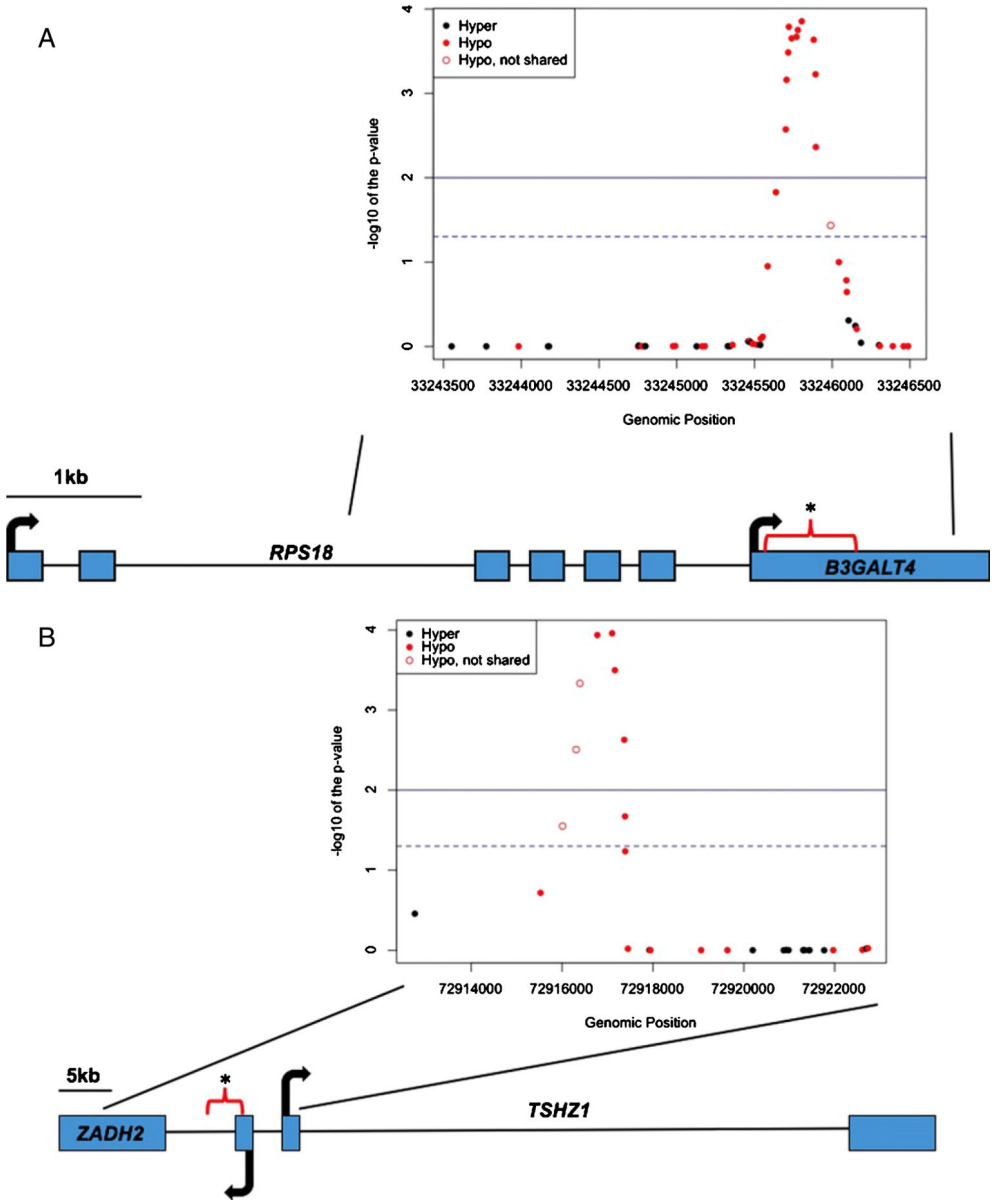


**Fig. 2.**

Relative positions of LOAD versus no-LOAD differentially methylated positions (DMPs) at *B3GALT4* and *ZADH2* loci. A) (Upper panel) Schematic of *B3GALT4* and its neighboring gene *RSP18.* The relative positions of probes measuring methylation levels of CpG sites annotated to *B3GALT4* with their genomic 5'−3' positions are provided (inset panel; x-axis) versus the -$\log_{10}$ of the adjusted local index of significant (aLIS) *p*-value (y-axis). All probes were tested for hypermethylation (black dots) and hypomethylation (red dots). Levels of aLIS *p*-values <0.05 (dashed blue line) and <0.01 (continuous blue line) are displayed. In the LOAD versus. no-LOAD comparison, 13 hypomethylated probes ($n$ =13 exonic probes) exhibit an aLIS *p*-value <0.05. Their relative locations are highlighted by a red bracket and asterisk. The CpG IDs of the 12 probes with DMPs in *B3GALT4* in all 7 comparisons are: cg03127244, cg22878489, cg03721978, cg09349343, cg17103217, cg23950233,

cg21618521, cg19882268, cg00052772, cg27147350, cg06362282, cg24605046. The LOAD versus no-LOAD CpG DMP site cg26055446 was not shared between the 7 comparisons (hollow red dot). B) (Lower panel) Schematic of *ZADH2* and its neighboring gene TSHZ1. The relative positions of probes measuring methylation levels of CpG sites annotated to *ZADH2* with their genomic 5'−3' positions are provided (inset panel; x-axis) versus the $-\log_{10}$ of the aLIS *p*-value (y-axis). All probes were tested for hypermethylation (black dots) and hypomethylation (red dots). Levels of aLIS *p*-values <0.05 (dashed blue line) and <0.01 (continuous blue line) are displayed. In the LOAD versus no-LOAD comparison, 8 hypomethylated probes ($n = 5$ intronic, $n = 3$ exonic) exhibit an aLIS *p*-value <0.05. Their relative locations are highlighted by a red bracket and an asterisk. The CpG IDs of the 5 probes with DMPs in *ZADH2* in all 7 comparisons are: cg02750262, cg18449964, cg03972071, cg07889413, cg22088248. The LOAD versus no-LOAD CpG DMP sites cg21786191, cg21330207, and cg11568697 were not shared between the 7 comparisons (hollow red dots).

**Table 1**

Sample and biomarker characteristic means and standard deviations in parentheses

| | LOAD | No-LOAD | *T*-test or chi-square |
|---|---|---|---|
| N | 45 | 39 | |
| Age (y) | 73.56 (6.8) | 75.33 (6.0) | $t$=−1.27, $p$=0.21 |
| Sex | 22 M; 23 F | 18 M; 21 F | $\chi^2$ =0.06, $p$=0.80 |
| Education (y) | 14.6 (2.3) | 16.6 (3.0) | $t$=3.32, $p$=0.001 |
| $A\beta_{42}$ (ln) [1] (pg/mL) | 6.02 (0.4) | 6.65 (0.3) | $t$=5.56, $p$<0.001 |
| $A\beta_{42}/A\beta_{40}$ [1] (pg/mL) | 0.06 (0.02) | 0.10 (0.02) | $t$=4.66, $p$<0.001 |
| t-tau [1] (pg/mL) | 806.67 (361.7) | 454.11 (199.0) | $t$=−3.56, $p$=0.002 |
| p-$tau_{181}$ [1] (pg/mL) | 79.84 (29.0) | 56.6 (19.9) | $t$=−3.01, $p$=0.005 |
| t-tau/$A\beta_{42}$ [1] (pg/mL) | 2.05 (0.9) | 0.64 (0.4) | $t$=−5.98, $p$<0.001 |
| p-$tau_{181/}$ $A\beta_{42}$ [1] (pg/mL) | 0.20 (0.1) | 0.08 (0.1) | $t$=−6.02, $p$<0.001 |

[1] CSF sample $n$=40 ($n$=16 LOAD and $n$ = 24 no-LOAD controls).